Mattice, W. L., Riser, J. M., & Clerk, D. S. (1976) *Biochemistry 15*, 4264–4272.
Moran, E. C., Chou, P. Y., & Fasman, G. D. (1977) *Biochem. Biophys. Res. Commun. 77*, 1300–1306.
Reynolds, J. A., & Tanford, C. (1970) *Proc. Natl. Acad. Sci. U.S.A. 66*, 1002–1007.
Sasaki, K., Dockerill, S., Adamiak, D. A., Tickle, I. J., & Blundell, T. (1975) *Nature (London) 257*, 751–757.
Satake, I., & Yang, J. T. (1976) *Biopolymers 14*, 1841–1846.
Schneider, A. B., & Edelhoch, H. (1972) *J. Biol. Chem. 247*, 4992–4995.
Srere, P. A., & Brooks, G. C. (1969) *Arch. Biochem. Biophys. 129*, 708–710.
Steinhardt, J., Stocker, N., Carroll, D., & Birdi, K. S. (1974) *Biochemistry 13*, 4461–4468.
Thomsen, J., Kristiansen, K., Brunfeldt, K., & Sundby, F. (1972) *FEBS Lett. 21*, 315–319.
Visser, L., & Blout, E. R. (1971) *Biochemistry 10*, 743–752.
Weber, K., & Osborn, M. (1969) *J. Biol. Chem. 244*, 4406–4412.
Wu, C.-S. C., & Yang, J. T. (1978) *Biochem. Biophys. Res. Commun. 78*, 914–919.
Yang, J. T., & Wu, C.-S. C. (1978) in *Versatility of Proteins* (Li, C. H., Ed.) pp 99–118, Academic Press, New York.
Yang, J. T., Bewley, T. A., Chen, G. C., & Li, C. H. (1977) *Proc. Natl. Acad. Sci. U.S.A. 74*, 3235–3238.

Proton Nuclear Magnetic Resonance Studies on Dideoxyribonucleoside Methylphosphonates†

Lou S. Kan,* Doris M. Cheng, Paul S. Miller, Junichi Yano, and Paul O. P. Ts'o

ABSTRACT: A series of dideoxyribonucleoside methylphosphonates, d-A*p*A, d-A*p*T, d-T*p*A, and T*p*T, were synthesized chemically and the diastereoisomers of each dimer were separated [Miller, P. S., Yano, J., Yano, E., Carroll, C., Jayaraman, K., & Ts'o, P. O. P. (1979) *Biochemistry 18*, 5134]. The ^{1}H NMR spectra of these compounds are similar to those of their parent diester compounds. Specifically, the assignments of the ^{1}H resonances of the two diastereoisomers of d-A*p*A (designated as 1 and 2) were reaffirmed by comparing with the unmodified, parent d-ApA. The absolute configuration of the phosphonate methyl group of the two isomers (d-A*p*A)$_1$ and (d-A*p*A)$_2$ was determined by the NOE technique. The ^{1}H NMR spectra of the diastereoisomers of d-A*p*A, as well as the corresponding monomer components d*A*p and CH_3*p*dA, and T*p*T were analyzed by spectrum simulation techniques. Thus, all the coupling constants and chemical shifts of the proton resonances of the deoxyribofuranose ring and the phosphonate methyl group could be precisely determined. These data provide the information for an analysis of the sugar puckering and backbone conformations of these novel nonionic nucleic acid analogues. It was found that the conformations of the sugar–phosphate backbones of each isomer are similar to each other and are similar to the conformations of the parent dinucleoside monophosphates. The average adenine stacking conformations of (d-A*p*A)$_1$ and (d-A*p*A)$_2$ were described in numerical coordinates derived from a computer analysis which included both ring-current magnetic anisotropy and atomic diamagnetic anisotropy effects. The two computer-derived conformational models are similar to those derived from the graphic approximation based only on the ring-current effects. For each pair of dimer analogues, the base stacking mode of isomer 1 is similar to that of its parent diester while the extent of base overlap in isomer 2 is less than that in isomer 1. The results of the conformational analysis based on NMR data are consistent with the results obtained from ultraviolet and circular dichroism measurements on these dimers.

Recently we described the synthesis of a series of deoxyribonucleoside methylphosphonates (Miller et al., 1979b). These nonionic nucleic acid analogues contain a 3′–5′ methylphosphonyl internucleoside linkage in place of the naturally occurring 3′–5′ phosphodiester linkage. These analogues not only serve as useful models for studying the conformational properties of nucleic acids (Miller et al., 1979b) but they can also serve as probes of nucleic structure and function within living cells (Miller et al., 1979a). This is because these nonionic analogues are very resistant to nucleases and enter the living mammalian cells with ease. The conformational properties of the individual diastereoisomers of each dimer, which differ only in the configuration of the phosphonate methyl group, were examined by UV and CD spectroscopy. The results of these studies suggested that each diastereoisomer has a distinct conformation in solution. This conclusion was further supported by the finding that the diastereoisomers of the dideoxyadenosine methylphosphonates each form complexes with poly(uridylic acid) having unique melting temperatures.

The detailed conformation of these dimers in solution has been studied by ^{1}H NMR[1] spectroscopy, including spin simulation, sequential-selective decoupling, nuclear Overhauser effects, and conformational model analyses by computer programs. In this paper, the ^{1}H NMR data are used to derive the conformation of each diastereoisomer of each dideoxyribonucleoside methylphosphonate, and the results are com-

† From the Division of Biophysics, School of Hygiene and Public Health, The Johns Hopkins University, Baltimore, Maryland 21205. *Received September 19, 1979.* This work was supported by a grant from the National Institutes of Health (GM016066-11) and a grant from the National Science Foundation (PCM77-25226). This paper was presented in part at the 1978 Biophysics Annual Meeting, Washington, DC.

[1] Abbreviations used: d-N*p*N, a deoxyribonucleotide dimer analogue containing a 3′–5′ internucleoside methylphosphonate linkage; (d-N*p*N)$_{1+2}$, a mixture of two stereoisomers of d-N*p*N; (d-N*p*N)$_{1and2}$, two individual compounds, i.e., (d-N*p*N)$_1$ and (d-N*p*N)$_2$; NMR, nuclear magnetic resonance; NOE, nuclear Overhauser effect; DSS, 2,2-dimethyl-2-silapentane-5-sulfonate; d-ApA, deoxyadenylyl(3′–5′)deoxyadenosine; poly(U), poly(uridylic acid).

0006-2960/80/0419-2122$01.00/0

Table I: Chemical Shifts (δ) of Base, $H_{1'}$, and PCH_3 Proton Resonances of (d-N*p*N′)$_n$ (in ppm from DSS) in 0.01 M Phosphate Buffer, pH 6.5

compd	concn (mM)	temp (°C)	chemical shifts: Np– H_8 (H_6)	Np– H_2 (CH_3)	Np– $H_{1'}$	–pN′ H_8 (H_6)	–pN′ H_2 (CH_3)	–pN′ $H_{1'}$	PCH_3[a]
(d-A*p*A)$_1$	12	6	7.94	7.74	6.05	8.22	7.95	6.22	1.69
		26	7.99	7.84	6.09	8.22	8.03	6.27	1.68
		45	8.00	7.89	6.10	8.20	8.05	6.30	1.64
		75	8.05	8.00	6.17	8.20	8.12	6.35	1.63
(d-A*p*A)$_2$	9	4.3	7.94	7.87	5.94	8.28	8.04	6.31	1.72
		14	8.00	7.90	5.97	8.25	8.05	6.31	1.69
		30	8.08	7.98	6.05	8.26	8.10	6.36	1.69
		49	8.12	8.04	6.12	8.25	8.12	6.38	1.66
		73	8.14	8.11	6.19	8.23	8.16	6.40	1.62
(d-A*p*T)$_1$	11	6	8.21	8.08	6.37	7.31	1.59	6.10	1.73
		26	8.24	8.14	6.39	7.33	1.64	6.13	1.73
		45	8.22	8.16	6.39	7.34	1.67	6.13	1.71
		75	8.23	8.20	6.41	7.37	1.73	6.16	1.71
(d-A*p*T)$_2$	13	2.3[b]	8.25	8.19	6.43	7.44	1.75	6.24	1.77
		25[b]	8.27	8.21	6.45	7.43	1.78	6.26	1.74
		30[b]	8.26	8.21	6.44	7.43	1.79	6.26	1.74
		45	8.24	8.19	6.42	7.38	1.78	6.24	1.71
		75	8.24	8.21	6.42	7.36	1.80	6.25	1.71
(d-T*p*A)$_1$	5	6	7.29	1.81	5.94	8.32	8.07	6.36	1.58
		25	7.32	1.84	5.95	8.32	8.13	6.41	1.59
		45	7.31	1.83	5.96	8.28	8.14	6.41	1.56
		75	7.35	1.85	6.11	8.27	8.20	6.43	1.56
(d-T*p*A)$_2$	5	6	7.41	1.81	5.86	8.31	8.12	6.36	1.58
		25	7.43	1.84	5.95	8.31	8.17	6.41	1.59
		45	7.41	1.83	5.96	8.27	8.18	6.41	1.56
		75	7.43	1.85	6.11	8.26	8.23	6.43	1.57
(T*p*T)$_1$	20	6	7.49	1.83	6.23	7.57	1.83	6.26	1.68
		26	7.48	1.84	6.24	7.54	1.84	6.26	1.69
		45	7.44	1.83	6.21	7.50	1.83	6.24	1.66
		75	7.41	1.84	6.22	7.47	1.84	6.25	1.66
(T*p*T)$_2$	3	6	7.50	1.86	6.24	7.59	1.86	6.28	1.70
		26	7.49	1.86	6.24	7.57	1.86	6.28	1.70
		45	7.45	1.85	6.23	7.53	1.85	6.27	1.68
		75	7.43	1.86	6.23	7.50	1.86	6.26	1.68

[a] The coupling constant of J_{PCH_3} is a constant (17.6 Hz) for all d-N*p*N′-type compounds. [b] Saturated solution.

pared with the conformation of the parent dimer containing the naturally occurring phosphodiester linkage and analogous dideoxyribonucleotide methyl and ethyl phosphotriesters (Miller et al., 1971; Kan et al., 1973a). In the case of the deoxyadenosine dimer d-A*p*A, the absolute configuration of the methylphosphonate group for each diastereoisomer was assigned by NOE techniques. The configuration of the methylphosphonate group was found to exert an influence on the stacking configuration of the isomers, particularly in the case of (d-A*p*A)$_1$ vs. (d-A*p*A)$_2$. The NMR results are in agreement with those obtained from the UV absorption spectroscopy and CD studies reported earlier (Miller et al., 1979b).

In this paper and in the supplementary material (see paragraph at end of paper regarding supplementary material), we have also introduced a computer analysis of the NMR data for the stacking conformation of the adenine dimers. In this computer program, both ring-current magnetic anisotropy and the atomic diamagnetic anisotropic effects are included in the calculation, and the computer results of the relative positions of the two bases can be described by numerical coordinates.

Experimental Section

Materials. The synthesis and separation of the diastereoisomers of the four dideoxyribonucleoside methylphosphonates d-A*p*A, d-A*p*T, d-T*p*A, and T*p*T and the syntheses of the monodeoxyribonucleoside methylphosphonates d*Ap*, T*p*, CH_3*p*dA, and CH_3*p*T were described previously (Miller et al., 1979b). d-ApA was obtained from Sigma Chemical Co., St. Louis, MO.

^{1}H NMR Measurements. All NMR samples were lyophilized twice with 99.8% D_2O (Bio-Rad Inc.) and then dissolved in 0.01 M phosphate buffer in D_2O at pH 6.5. The concentrations of each sample are listed in Tables I and II. The ^{1}H NMR spectra were obtained on three different NMR Fourier transform spectrometers. The chemical shifts (δ) of the base protons, PCH_3 protons, and $H_{1'}$ resonances of all dimers were obtained on a Varian HR-220 NMR spectrometer. In addition, monomers and dimers of d-A*p*A and T*p*T were measured on a Bruker WH 360 NMR spectrometer as well. All chemical shifts were measured with DSS as the reference, as described by Cheng et al. (1980). The NOE measurements of the PCH_3 group of (d-A*p*A)$_{1and2}$ were performed on a JEOL FX-100 NMR spectrometer. The intensity of the PCH_3 resonance was measured with respect to the intensities of the base protons as reference with and without irradiation of the H-3′ resonance of the d*Ap*– unit of the dimer. The measurement of the intensity was based on signal height and was accurate to ±1%. Spectrum simulation was performed on a JEOL 980 minicomputer with JEOL simulation software.

Results and Discussion

Assignment of Proton Resonances. The proton resonances of the mono- and dideoxyribonucleoside methylphosphonates

Table II: Chemical Shifts (δ) of Base, H_1', $POCH_3$, and PCH_3 Proton Resonances of dA*p*, T*p*, CH_3*p*dA, and $(CH_3pT)_1$ (in ppm from DSS) in 0.01 M Phosphate Buffer, pH 6.5

compd	concn (mM)	temp (°C)	chemical shifts				
			H_8 (H_6)	H_2 (CH_3)	H_1'	$POCH_3$	PCH_3
dA*p*	9	6	8.27	8.14	6.46		1.33[a]
		26	8.30	8.20	6.48		1.33
		45	8.28	8.20	6.45		1.34
		75	8.29	8.24	6.46		1.32
T*p*	15	6	7.65	1.87	6.32		1.29[a]
		26	7.63[b]	1.87[b]	6.30		1.30
		45	7.60	1.86	6.27		1.28
		75	7.59	1.88	6.25		1.29
$(CH_3pdA)_{1+2}$ mixture	13.5 total	3.5	8.30	8.16	6.43	3.55[e] (s)[d]	1.40[f]
					(6.1)[c]	3.44 (l)[d]	1.41
		14.5	8.30	8.19	6.44	3.56 (s)	1.40
					(6.0)	3.45 (l)	1.42
		24.7	8.28	8.19	6.43	3.55 (s)	1.40
					(5.7)	3.45 (l)	1.41
		39.2	8.30	8.24	6.47	3.58 (s)	1.42
					(6.3)	3.50 (l)	1.44
		60.0	8.28	8.25	6.47	3.59 (s)	1.43
					(6.1)	3.53 (l)	1.45
		75.1	8.27	8.27	6.47	3.61 (s)	1.44
					(6.5)	3.54 (l)	1.46
$(CH_3pT)_1$	47.5	3.5	7.55	1.89	6.32	3.75[e]	1.63[f]
		14.5	7.54	1.89	6.31	3.74	1.62
		24.7	7.52[b]	1.89[b]	6.29	3.74	1.62
		39.2	7.52	1.89	6.30	3.75	1.63
		60	7.50	1.88	6.27	3.75	1.63
		75.1	7.49	1.89	6.27	3.75	1.62

[a] The coupling constant of J_{PCH_3} is equal to 16.6 Hz and kept as a constant through the temperature range. [b] The coupling constant between C_6-H and C_5-CH_3 can be detected (1-1.2 Hz) from this temperature and up. [c] Approximate values for $J_{1'2'}$ and $J_{1'2''}$ in these compounds. [d] CH_3*p*dA is a mixture of its diastereoisomers. Only H_3, H_2, and H_1' resonances showed a single set of peaks of these two diastereoisomers. Other protons, including $POCH_3$ and PCH_3, have two sets of signals: one set with smaller intensity (s) (~40%) and another set with larger intensity (l) (~60%). [e] The three-bond coupling constant between P and H is a constant (11.2 Hz). [f] The two-bond coupling constant between P and H is also a constant (17.6 Hz).

can be divided into three categories for purposes of assignment.

(*1*) *PCH_3 Resonances.* This signal can be easily located and assigned by its characteristic coupling with ^{31}P ($^2J_{PH}$ = 17.6 or 16.6 Hz) and by its large intensity (three protons) in dA*p* and d-A*p*A. This signal is readily distinguished from the thymine methyl resonances in T*p*, d-A*p*T, d-T*p*A, and T*p*T since the T–CH_3 resonance occurs as a doublet with a coupling constant of ~1 Hz to the H_6 proton of the base. The assignment of the PCH_3 resonances in $(CH_3pdA)_{1and2}$ and $(CH_3pT)_1$ is straightforward since the J_{PCH_3} (16.3–17.6 Hz) value agrees with the data obtained from ^{31}P NMR measurements (L. S. Kan et al., unpublished experiments). This value is larger than the value of J_{POCH_3} (11.2 Hz; Table II, footnote *f*). Chemical shift assignments are shown in Figure 1 and Tables I and II.

(*2*) *Base Proton Resonances.* (*a*) *$(d\text{-}ApA)_1$ and $(d\text{-}ApA)_2$.* Unlike the two diastereoisomers of d-Ap(Et)A (Miller et al., 1971), the chemical shifts of base proton resonances of the two diastereoisomers of d-A*p*A are slightly different (0.01–0.09 ppm) even at moderately high temperature (Table I and Figure 1a,b). For this reason, the assignment of these resonances was carefully evaluated by comparison with the previously assigned chemical shifts of base protons of d-ApA (Kondo et al., 1972). The chemical shift data of these three dimers vs. temperatures are shown in Figure 2. According to the previous assignment from our laboratory (Kondo et al., 1972), the resonances at 8.30 ppm and at 8.13 ppm belong to H_8 and H_2 of –pdA, respectively, and resonances at 8.06 and 8.02 ppm belong to H_8 and H_2 of dAp–, respectively, at 75 °C (Figure 2). The results of relaxation experiments are relevant to these assignments; namely, resonances at 8.30 and 8.06 ppm have relatively shorter spin–lattice relaxation times (characteristic of H_8 resonance due to the closer proximity to the protons of the furanose ring), while resonances at 8.13 and 8.02 ppm have longer relaxation times (characteristic of H_2 resonances) (Ts'o et al., 1973). For $(d\text{-}ApA)_1$, there are also four separate resonances. The chemical shifts of three signals not only have similar values to those of H_2 of –pdA and H_8 and H_2 of dAp– at high temperature but also have similar temperature dependence properties to these three signals from d-ApA (Figure 2). In addition, the resonance at 8.07 ppm [which is nearly identical with the chemical shift (8.06 ppm) of H_8 of dAp– in d-ApA] of $(d\text{-}ApA)_1$ also has a shorter T_1 value. Therefore, the signal at 8.07 ppm of $(d\text{-}ApA)_1$ can be assigned to H_8 of the dA*p*– residue according to the previous procedure. By the similarity in chemical shifts, the resonances at 8.15 and 8.02 ppm are assigned to H_2's of –*p*dA and dA*p*– of $(d\text{-}ApA)_1$, respectively. The remaining resonance at 8.23 ppm which also has a shorter T_1, therefore, can be assigned to H_8 of –*p*dA of $(d\text{-}ApA)_1$. This signal is shifted ~0.07 ppm further upfield than H_8 of -pdA in d-ApA. This may be due to the absence of the deshielding effect of the negative charge of phosphate eliminated by the –CH_3 group. A similar effect of shielding was also observed in the d-Ap(Et)A triester (Miller et al., 1971). In addition, this resonance showed a temperature dependence very similar to that of the H_8 of –pdA in d-ApA. Therefore, the assignment of the base proton resonances of $(d\text{-}ApA)_1$ can be made with relative certainty. Furthermore, this result also provides the information that the stacking conformation of $(d\text{-}ApA)_1$ is closely similar to that of d-ApA.

There are also four separated signals in the spectrum of $(d\text{-}ApA)_2$. However, their chemical shift values are different

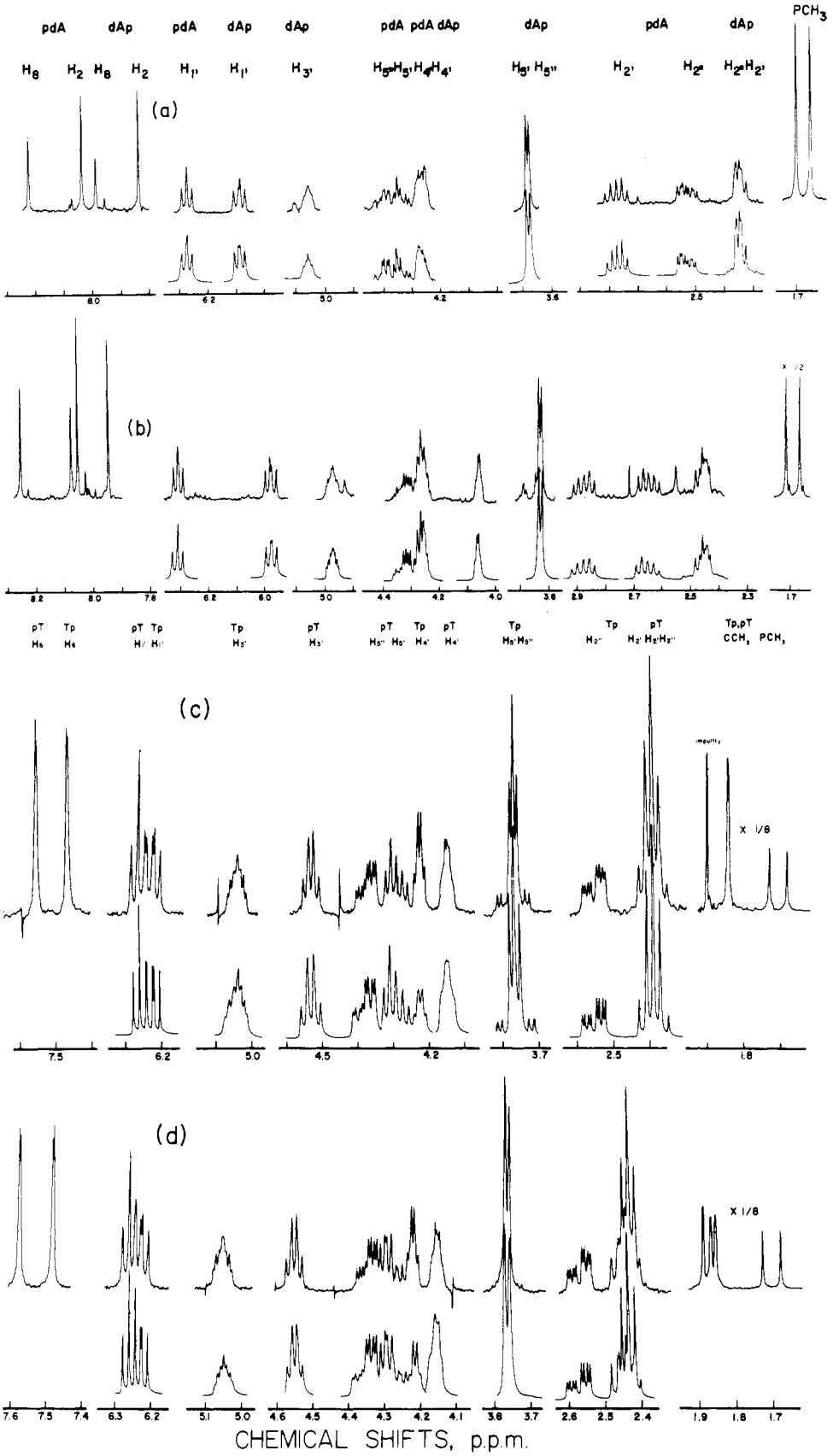

FIGURE 1: 360-MHz spectra of d-A*p*A and T*p*T at 25 °C, D_2O, and neutral pH. The simulated spectra of furanose proton resonances are shown below the experimental spectra for (a) (d-A*p*A)$_1$, (b) (d-A*p*A)$_2$, (c) (T*p*T)$_1$, and (d) (T*p*T)$_2$. The precise chemical shift data of each resonance are described in Tables I and IV.

from those of (d-A*p*A)$_1$. The signal at 8.25 ppm can be assigned to H_8 of –*p*dA of (d-A*p*A)$_2$ because it has a short T_1 and a spectral position between those of the resonances of H_8 of –*p*dA of (d-A*p*A)$_1$ and H_8 of –pdA of d-ApA but far away from those of H_8 of dAp– of d-ApA or (d-A*p*A)$_1$. The remaining three signals of (d-A*p*A)$_2$ cannot be matched to the

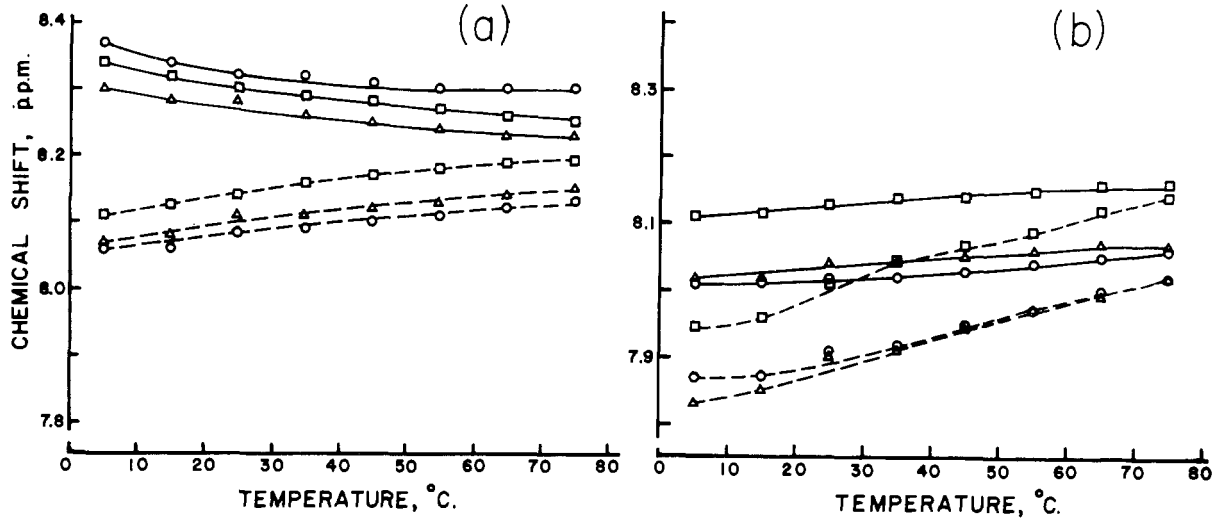

FIGURE 2: Temperature dependence of the chemical shifts of the base proton resonances of d-ApA (○), (d-A*p*A)$_1$ (△), and (d-A*p*A)$_2$ (□). The solid lines represent the H_8 resonances and the broken lines represent the H_2 resonances. (a) The 5′-residual portion (–pA); (b) the 3′-residual portion (Ap–).

resonances of d-ApA directly at high temperature. However, the signal at 8.16 ppm has a shorter T_1 than those of the other two (8.19 and 8.14 ppm). Therefore, this resonance can be assigned to the H_8 of dA*p*– of (d-A*p*A)$_2$. The signal at 8.14 ppm is shifted to 7.94 ppm at low temperature (5 °C); the temperature dependence of this signal is similar to that of H_2 of dAp– in d-ApA [and (d-A*p*A)$_1$] (Figure 2). Therefore, this resonance at 8.14 ppm (at 75 °C) can be assigned to H_2 of dA*p*– in (d-A*p*A)$_2$. Thus, the remaining signal at 8.19 ppm belongs to the H_2 resonance of –*p*dA in (d-A*p*A)$_2$.

These assignments indicate that there is a general pattern of base proton resonances in all three dA dimers at high temperature. Namely, all H_8's of –*p*dA have the greatest downfield chemical shift; next is H_2 of –*p*dA, then H_8 of dA*p*–, and finally H_2 of dA*p*– which has the greatest upfield chemical shift. This pattern is very useful for the assignment of $H_{1'}$ on the furanose ring.

(*b*) *(TpT)$_1$ and (TpT)$_2$.* The differences between the chemical shifts of the base proton resonances in the two T*p*T diastereoisomers are small [up to 0.09 ppm for the H_6 signal at 6 °C and 0 ppm for C_5 and CH_3 signals (Table I)]. Therefore, the assignment of these signals is not critical for the conformation analysis. Since the base proton resonances of the two d-A*p*A diastereoisomers have a pattern similar to that of d-ApA, it is reasonable to expect that the base proton resonances of T*p*T are similar to those of TpT. For this reason, the H_6 and C_5–CH_3 resonances of (T*p*T)$_1$ and (T*p*T)$_2$ can be assigned readily in accordance to the known assignment of the resonances of TpT (Table I).

(*c*) *d-TpA and d-ApT Diastereoisomers.* The assignment of base proton resonances of these four heterodideoxyribonucleoside methylphosphonates is simple because of the different characteristics of each signal. For example, H_8 and H_2 of the adenine residue are singlets, while H_6 is a doublet with a very small coupling constant. It is interesting to note here that all these methylphosphonate dimers have similar resonance patterns to their parent diester compounds [Table I and Kan et al. (1973b)].

(*3*) *Deoxyribofuranose Proton Resonances.* The assignment of the $H_{1'}$ resonance of the dideoxyribonucleoside methylphosphonates is patterned after their parent diesters. This approach is based on the same reasoning as stated in section 2a. Once the $H_{1'}$ resonance was established, the other sugar proton resonances of dA*p*, T*p*, (CH$_3$*p*T)$_1$ (d-A*p*A)$_{1and2}$, and (T*p*T)$_{1and2}$ were assigned by systematic decoupling starting from the assigned $H_{1'}$ (Cheng & Sarma, 1977). The assignments are shown in Figure 1 and Table III.

General Description of the ^1H NMR Data on Mono- and Dideoxyribonucleoside Methylphosphonates. The base protons, PCH_3 protons, and $H_{1'}$ resonances of each diastereoisomer of the dideoxyribonucleoside methylphosphonates are listed in Table I. The differences in chemical shift between the diastereoisomers of each dimer are relatively small at low temperature and become negligible as the temperature increases. For a pair of diastereoisomers, the base proton signals in isomer 1 are shifted further upfield than the corresponding resonances in isomer 2. The magnitude of this upfield shift depends upon the nature of the base in the dimer, i.e., 0.03–0.13 ppm in d-A*p*A, 0.04–0.16 ppm in d-A*p*T, 0.0–0.12 ppm in d-T*p*A, and 0.01–0.03 ppm in T*p*T at low temperature.

Like the base protons, most of the $H_{1'}$ proton resonances of isomer 1 occur at higher field than those of isomer 2. Two exceptions are the $H_{1'}$ resonances of the dN*p* units of (d-A*p*A)$_1$ and (d-T*p*A)$_1$, which are shifted downfield 0.09 and 0.08 ppm, respectively, relative to the resonances in (d-A*p*A)$_2$ and (d-T*p*A)$_2$. These two dimers have a common base, dA, in the –*p*dN unit of the dimer. Therefore, this observation may reflect a difference in the base stacking mode between isomer 1 and isomer 2. This point will be discussed in greater detail in the following section.

The PCH_3 resonances are doublets with a hetero coupling constant, $^2J_{PH}$, of 17.6 Hz and with chemical shifts between 1.56 and 1.74 ppm. There is a very small difference (up to 0.03 ppm) in the chemical shifts of the methyl resonances between the two diastereoisomers for each dimer. The chemical shift of the PCH_3 resonance occurs at higher field in isomer 1 than that in isomer 2. For both diastereoisomers, the PCH_3 resonance shifts upfield with increasing temperature. This upfield shift may result from the increased shielding of the methyl groups by the bases, as the bases begin to oscillate out of the stacked conformation (Kan et al., 1973a).

Since the dideoxyribonucleoside methylphosphonates are uncharged in aqueous solution at neutral pH, deoxyribonucleoside monophosphates cannot be used to calculate dimerization shifts ($\Delta\delta$). Therefore, CH$_3$*p*dA and CH$_3$*p*T were used to calculate $\Delta\delta$ of the –*p*dN unit of each dimer. In these compounds the methyl ester group does not exert any ring-current shielding effects, but it does eliminate the negative

Table III: Chemical Shifts (δ) of All the Sugar Proton Resonances except $H_{1'}$ of d*Ap*, T*p*, $(CH_3pT)_1$, (d-A*p*A)$_{1\text{and}2}$, and (T*p*T)$_{1\text{and}2}$ in D_2O (in ppm from DSS)

		chemical shifts											
		dN*p*–						–*p*dN′					
compd	temp (°C)	2′	2″	3′	4′	5′	5″	2′	2″	3′	4′	5′	5″
d*Ap*	26	2.41	2.49	*a*	4.14	3.84	3.78						
	75	2.39	2.48	4.76	*a*	3.82	3.78						
T*p*	26	2.88	2.67	4.95	4.31	3.84	3.81						
	75	2.87	2.69	4.94	*a*	3.83	3.78						
$(CH_3pT)_1$	26							2.40	2.42	4.56	4.17	4.24	4.30
	75							2.36	2.41	4.52	4.15	4.23	4.29
(d-A*p*A)$_1$	26	2.33	2.36	5.06	4.26	3.69	3.68	2.78	2.53	*a*	4.28	4.34	4.41
	75	2.46	2.42	5.03	*a*	3.68	3.65	2.81	2.56	4.68	4.24	4.29	4.33
(d-A*p*A)$_2$	26	2.46	2.43	4.97	4.06	3.63	3.62	2.87	2.64	*a*	4.28	4.27	4.33
	75	2.63	2.51	4.99	4.08	3.63	3.61	2.86	2.62	4.73	*a*	4.23	4.29
(T*p*T)$_1$	26	2.39	2.55	5.04	4.22	3.79	3.76	2.39	2.39	4.53	4.14	4.29	4.38
	75	2.37	2.51	5.01	4.16	3.76	3.72	2.33	2.36	4.45	4.10	4.22	4.30
(T*p*T)$_2$	26	2.43	2.55	5.06	4.22	3.77	3.76	2.42	2.42	4.56	4.15	4.28	4.34
	75	2.42	2.53	5.01	4.17	3.76	2.73	2.36	2.39	4.48	4.12	4.24	4.29

[a] The signal is under the HDO peak.

charge of the phosphonate group. The $\Delta\delta$ of the dN*p*– unit in each dimer was calculated by using the 3′-nucleosidyl methylphosphonates d*Ap* and T*p* as references. Although these monomers carry a single negative charge at neutral pH, it is known from previous studies that a phosphate group at the 3′-OH position has a very small effect on the base and $H_{1'}$ proton resonances of the nucleotide (Ts'o et al., 1969).

The chemical shift values of the base, $H_{1'}$, and PCH_3 protons of d*Ap*, T*p*, $(CH_3pdA)_{1+2}$, and $(CH_3pT)_1$ are listed in Table II. Although the CH_3pdA sample consisted of a mixture of two diastereoisomers, the base and $H_{1'}$ resonances of each diastereoisomer had the same chemical shift over the temperature range studied. This indicates that the magnetic environment of the base and $H_{1'}$ protons is very similar for each isomer. However, the other furanose proton signals as well as the $POCH_3$ and PCH_3 resonances have slightly different chemical shifts. The sugar multiplet signals are too complex to analyze. On the other hand, the $POCH_3$ and PCH_3 resonances of each isomer can be distinguished. The intensities of one set of $POCH_3$ and PCH_3 resonances (designated as "s" in Table II) are slightly smaller than the other set (designated as "l" in Table II), indicating that the ratio of the diastereoisomers in the mixture is not 1:1. The chemical shifts of the base, $H_{1'}$, $POCH_3$, and PCH_3 proton resonances of the monomers are essentially independent of temperature. This is due to the low concentration used in the NMR measurements which results in little or no intermolecular interaction.

The $^2J_{PH}$ values of d*Ap* and T*p* are 16.6 Hz while those of $(CH_3pdA)_{1+2}$ and $(CH_3pT)_1$ are 17.6 Hz. The latter values are very similar to the $^2J_{PH}$ values observed for the dimers (see Table I). This observation indicates that esterification of the oxygen of the nucleoside phosphonate group results in only small changes in the electron density at the phosphorus atom. The $^3J_{PH}$ value of $POCH_3$ in the monomers is 11.2 Hz, which is identical with that of the methyl phosphotriester, d-Ap-(CH_3)A (Miller et al., 1971).

The $\Delta\delta$ values of the base and $H_{1'}$ resonances of the dimers were calculated by using the formula $\Delta\delta = \delta$(dimer) – δ-(monomer) (Ts'o et al., 1969). Results are listed in Table IV. The data show that the $\Delta\delta$ values of the base and $H_{1'}$ proton resonances of isomer 1 are larger than those of isomer 2, particularly for d-A*p*A and d-A*p*T. This suggests that base overlap may be more extensive in isomer 1 than in isomer 2.

The effects of temperature on δ and $\Delta\delta$ of the dideoxyribonucleoside methylphosphonates are very similar to the effects on the corresponding dideoxyribonucleoside monophosphates (Kondo et al., 1972; Cheng & Sarma, 1977). In order to make a detailed comparison between the phosphonate analogues and the parent diesters, three monodeoxyribonucleoside methylphosphonates, d*Ap*, T*p*, and $(CH_3pT)_1$, and four dideoxyribonucleoside methylphosphonates, (d-A*p*A)$_{1\text{and}2}$ and (T*p*T)$_{1\text{and}2}$, were analyzed by spin simulation methods at 25 and 75 °C. Selected spectra accompanied by the simulated spectra are shown in Figure 1. This analysis enabled the chemical shifts and coupling constants of all the proton resonances to be accurately determined. Tables III and V show, respectively, the δ values in parts per million of the deoxyribofuranose proton resonances (except $H_{1'}$) and the coupling constant values (except $J_{C_6H-C_5CH_3}$ of thymine, $^2J_{PH}$, and $^3J_{PH}$ which have been reported in Tables I and II).

Knowledge of the chemical shifts of the $H_{3'}$ resonances in the dimer (d-A*p*A)$_{1\text{and}2}$ (Table III) allowed an NOE experiment to be performed on these dimers. At 26 °C, irradiation of the $H_{3'}$ of the dA*p*– unit of (d-A*p*A)$_1$ resulted in a 12% by height increase in the intensity of the PCH_3 resonance. A similar experiment with (d-A*p*A)$_2$ resulted in no apparent change in the PCH_3 signal. As described under Mode of Base Stacking, these results allow an assignment of the absolute configurations of the phosphonate methyl groups of the diastereoisomers of d-A*p*A.

Mode of Base Stacking. It is well documented that the dinucleoside monophosphates do not adopt a fixed conformation with respect to base stacking interactions even at temperatures as low as 0 °C. Most likely, the bases in the dimer oscillate and rotate with respect to one another. The amplitude of this oscillation increases with increasing temperature (Kan et al., 1973a). Nevertheless, an average base stacking mode of the dimers can be derived from the $\Delta\delta$ values obtained at low temperatures. Thus, as shown in Table IV, for the dinucleoside methylphosphonates the $\Delta\delta$ values of isomer 1 are larger than those of the same resonance in isomer 2, except in the case of (T*p*T)$_{1\text{and}2}$. This result indicates that the extent of base overlap in isomer 1 is greater than that in isomer 2. A similar conclusion was reached based on the results of UV hypochromicity measurements on the deoxyadenosine containing dimers (d-A*p*A)$_{1\text{and}2}$ and (d-A*p*A*p*)$_{1\text{and}2}$

Table IV: Dimerization Shifts ($\Delta\delta$) in ppm of Base and $H_{1'}$ Proton Resonances of d-NpN'

		dimerization shifts					
		dNp–			–pdN'		
compd	temp (°C)	H_8 (H_6)	H_2 (CH_3)	$H_{1'}$	H_8 (H_6)	H_2 (CH_3)	$H_{1'}$
(d-ApA)$_1$	6	0.33	0.41	0.41	0.08	0.21	0.21
	26	0.31	0.37	0.39	0.05	0.16	0.16
	45	0.28	0.32	0.35	0.10	0.19	0.16
	75	0.24	0.25	0.29	0.07	0.15	0.13
(d-ApA)$_2$	4	0.33	0.27	0.52	0.02	0.12	0.13
	30	0.22	0.23	0.43	0.02	0.09	0.07
	49	0.16	0.16	0.34	0.05	0.12	0.08
	73	0.15	0.17	0.27	0.04	0.11	0.07
(d-ApT)$_1$	6	0.06	0.07	0.09	0.35	0.30	0.21
	26	0.06	0.06	0.08	0.18	0.24	0.16
	45	0.06	0.04	0.07	0.19	0.23	0.16
	75	0.06	0.07	0.09	0.12	0.16	0.16
(d-ApT)$_2$	6	0.02	–0.05	0.03	0.12	0.10	0.08
	25	0.03	0.00	0.03	0.09	0.11	0.04
	45	0.04	0.01	0.03	0.14	0.11	0.06
	75	0.05	0.03	0.04	0.12	0.09	0.02
(d-TpA)$_1$	6	0.36	0.06	0.37	–0.02	0.08	0.07
	26	0.36	0.03	0.34	–0.04	0.05	0.02
	45	0.29	0.04	0.30	0.02	0.09	0.06
	75	0.24	0.03	0.14	0.00	0.07	0.05
(d-TpA)$_2$	6	0.25	0.06	0.41	–0.01	0.04	0.07
	26	0.21	0.03	0.28	–0.03	0.01	0.02
	45	0.19	0.04	0.30	0.03	0.05	0.06
	75	0.15	0.03	0.14	0.01	0.04	0.05
(TpT)$_1$	6	0.16	0.04	0.09	–0.01	0.07	0.06
	26	0.16	0.03	0.06	–0.02	0.04	0.05
	45	0.16	0.04	0.06	0.02	0.06	0.06
	75	0.17	0.04	0.03	0.02	0.05	0.02
(TpT)$_2$	6	0.15	0.01	0.08	–0.04	0.04	0.04
	26	0.15	0.01	0.06	–0.05	0.02	0.03
	45	0.15	0.01	0.04	–0.01	0.04	0.03
	75	0.16	–0.01	0.02	–0.02	0.03	0.01

Table V: Comparison between the Observed and the Computed $\Delta\delta$ of Four Base Protons in (d-ApA)$_1$ and (d-ApA)$_2$ (the Computed Values Were Based on Conformational Models Constructed by the Computer Analyses)

			$\Delta\delta$			
			H_2		H_8	
			Ap–	–pA	Ap–	–pA
(d-ApA)$_1$:	computed	model I[a]	0.43	0.36	0.32	0.11
		model II[b]	0.47	0.23	0.34	0.18
	observed		0.41	0.21	0.33	0.08
(d-ApA)$_2$:	computed[c]		0.21	0.14	0.31	0.03
	observed		0.27	0.12	0.33	0.02

[a] $t_x = 0.4$ Å, $t_y = -1.3$ Å, $\theta_z = -10°$; $t_z = 3.2$ Å, θ_x and $\theta_y = 0°$. [b] $t_x = 0.4$ Å, $t_y = -1.3$ Å, $\theta_z = 1°$; $t_z = 3.2$ Å, θ_x and $\theta_y = 0°$. [c] $t_x = 1$ Å, $t_y = -2$ Å, $\theta_z = -1°$; $t_z = 3.2$ Å, θ_x and $\theta_y = 0°$.

(Miller et al., 1979b).

The base stacking modes of (d-ApA)$_{1and2}$, (d-TpA)$_{1and2}$, and (d-ApT)$_{1and2}$ are shown in Figure 3. These stacking modes were derived from the $\Delta\delta$ values of the dimers at 4 °C by using the isoshielding contours derived from the ring-current anisotropic shielding effect of the adenine and thymine bases (Giessner-Prettre et al., 1976). The stacking mode of (d-ApA)$_1$ is very similar, if not identical, to that of the corresponding diester, d-ApA. For example, in d-ApA $\Delta\delta$ values of H_8, H_2, and $H_{1'}$ of dAp– are 0.33, 0.31, and 0.42 and of –pdA are 0.16, 0.18, and 0.28 at 4 °C (Kondo et al., 1972).

The stacking mode of isomer 2 results from a slight clockwise rotation of the base of the –pdN unit with respect to the base dNp– unit. This rotation moves the high ring current region of the –pdN base away from the base protons of the dNp– unit but closer to the $H_{1'}$ proton of this unit. As a result, the $\Delta\delta$ values of the base protons in isomer 2 of d-ApA and d-TpA decrease while the $\Delta\delta$ values of the $H_{1'}$ protons increase compared to those in isomer 1. This rotation causes all the base and $H_{1'}$ protons of the –pdN unit to move away from the high ring current shielding region of the dNp– unit. Therefore, the $\Delta\delta$ values of the base and $H_{1'}$ protons of the –pdN unit in isomer 2 are smaller than those in isomer 1.

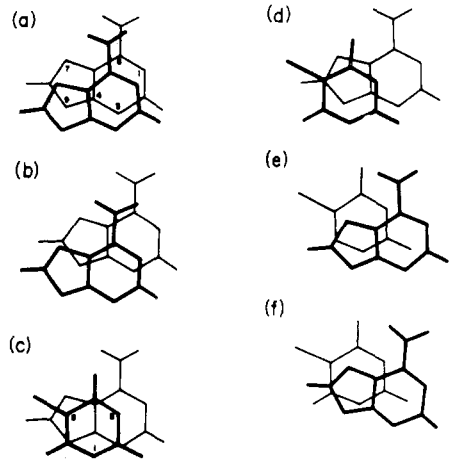

FIGURE 3: Schematic presentation of the conformational model of (a) (d-ApA)$_1$, (b) (d-ApA)$_2$, (c) (d-ApT)$_1$, (d) (d-ApT)$_2$, (e) (d-TpA)$_1$, and (f) (d-TpA)$_2$. The base in the 3'-nucleotidyl unit was drawn in thin lines and the base in the 5'-nucleotidyl unit was drawn in thick lines.

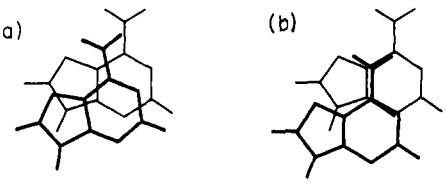

FIGURE 4: Schematic presentation of the conformational model of (a) (d-A*p*A)$_1$ and (b) (d-A*p*A)$_2$, based on the consideration of the $\Delta\delta$ values at 6 °C and the computer calculations of both ring-current and atomic diagmagnetic anisotropic effects (C. Giessner-Prettre, private communication). See the supplementary material for details. The adenine drawn with thin lines is the 3′-nucleotidyl unit and the adenine drawn with thick lines is the 5′-nucleotidyl unit.

The procedure used in arriving at the average conformation models shown in Figure 3 is based only on the graphic approximation of the ring-current magnetic anisotropy effect.

In order to perform a more precise computation of the relative position of two bases in a stacked dimer from chemical shift data, a computer program, which encompasses both ring-current magnetic anisotropy (Giessner-Prettre et al., 1976) and the atomic diamagnetic anisotropic effects (Giessner-Prettre & Pullman, 1968) and can calculate the relative positions of each atom in the two bases, was written[2] (supplementary material). The input data for this program are the Cartesian coordinates of each atom of the base, the atomic diamagnetic tensor of each atom of the base, and the intensity of ring current and thickness of the π electrons (C. Giessner-Prettre and B. Pullman, unpublished data). In this program, the two adenine bases are exactly superimposed on each other at the beginning, one base is held stationary, and the other base is rotated [about an arbitrary x, y, or z axis (θ_x, θ_y, or θ_z)] and then shifted (along x, y, and z axes) as desired. The program will calculate and print out the mutual shielding effect on every nucleus in the base in parts per million and atomic coordinates of both the fixed and the rotated/shifted bases. Therefore, this program can be used to search for a set of calculated shielding effects which will best fit the experimental NMR data by the rotating/shifting of one adenine base vs. the other. For (d-A*p*A)$_2$ at low temperature when the stacking model is built with the coordinates of the relative position between the stationary adenine and the moved adenine of $\theta_z = -1°$, $t_x = 1$ Å, $t_y = -2$ Å, $t_z = 3.2$ Å, and θ_x and $\theta_y = 0°$, the calculated $\Delta\delta$ values and the observed $\Delta\delta$ values are in very satisfactory agreement (Table V). For (d-A*p*A)$_1$ at low temperature, two conformational models are constructed with the following coordinates between the two adenines: model I, $\theta_z = -10°$, $t_x = 0.4$ Å, and $t_y = -1.3$ Å; model II, $\theta_z = 1°$, $t_x = 0.4$ Å, and $t_y = -1.3$ Å (again t_z is held at 3.2 Å; θ_x and $\theta_y = 0°$). The agreement is reasonable with a slight disagreement (0.15 ppm) in H_2 of –*p*dA for model I and a slight disagreement (0.10 ppm) in H_8 of –*p*dA for model II. At present, a choice between these two models cannot be made by ^{1}H NMR data alone. However, the CD data appear to favor model I, since the θ_z of model I (−10°) is larger than the θ_z of model II (1°), which may be a basis for the relatively large CD effect observed. Thus, tentatively, model I is adopted as shown in Figure 4. It is gratifying that the more precisely computed conformational models of (d-A*p*A)$_1$ and (d-A*p*A)$_2$ are not greatly different from those obtained by approximation mainly from the graphic approach based on the ring-current effect only.

The stacking modes of (d-A*p*A)$_{1and2}$ shown in Figures 3 and 4 are consistent with the CD spectra of these dimers described in our preceding paper (Miller et al., 1979b). Thus, for d-A*p*A, the electric dipole vectors of the base in isomer 2 are nearly parallel to each other ($\theta = -1°$), while in isomer 1 they are oblique ($\theta = -10°$). Since the magnitude of the CD rotation depends upon the angle between the dipole moment vector, the stacking modes depicted in Figures 3 and 4 would predict that isomer 2 should have a greatly diminished rotation relative to that of isomer 1. This is exactly the behavior which is observed for these dimers.

It is interesting to note that the base stacking mode of (d-A*p*A)$_1$ is very similar to that of d-ApA [Figure D in Kondo et al. (1972)], while that of isomer 2 shows less base–base overlap (Figures 3 and 4). The differences in the base stacking mode support the explanation given in the preceding paper for the melting behavior of (d-A*p*A)$_1$·poly(U) and (d-A*p*A)$_2$·poly(U) complexes (Miller et al., 1979b). The T_m of the (d-A*p*A)$_2$·poly(U) complex is higher than that of the (d-A*p*A)$_1$·poly(U) complex. Thus, the more open stack of isomer 2 can more easily adopt the A-type conformation of the poly(U) complex than can the more highly stacked isomer 1.

Conformation of the Sugar–Phosphate Backbone. The conformation of the deoxyribofuranose ring of these phosphonate dimers appears to favor the 2′-endo conformation, i.e., ^{2}E, with a phase angle of 144–180° (Sundaralingam, 1973). Cheng & Sarma (1977) have demonstrated that 59 out of 62 examined deoxyribose moieties have a constant sum of 10.8 ± 1 Hz for $J_{1',2'}$ and $J_{3',4'}$. From Table VI, the computed sums of $J_{1',2'}$ and $J_{3',4'}$ for the mono- and dideoxyribonucleoside methylphosphonates are in the range of 10.6–11.7 and 10.2–11.9 Hz, respectively. Therefore, by employing the sum of 10.8 Hz for $J_{1',2'}$ and $J_{3',4'}$ and the observed magnitude of $J_{3',4'}$ (Altona & Sundaralingam, 1973), the percentage population of ^{2}E conformers in the phosphonate compounds can be computed as shown in Table VII.

The sugar pucker of the three monodeoxyribonucleoside methylphosphonates, dA*p*, T*p*, and (CH$_3$*p*T)$_1$, is independent of changes in temperature. The ^{2}E populations of these monomers range from 74% (dA*p*) to 60% [(CH$_3$*p*T)$_1$] and are very similar to those of the parent monomers dAp, Tp, and pT (Table VII). Upon dimerization there is an increase in the ^{2}E population of the –*p*dN unit in both the deoxyadenosine- and thymidine-containing dimers. This effect may be due to the stacking influence of the adjacent dN*p*– unit. Comparison of dimers containing adenine vs. those containing thymine shows that thymidine in either the dN*p*– or –*p*dN unit has a lower percentge of ^{2}E population than deoxyadenosine. This observation reflects the lower stacking interactions of the thymine base compared to those of adenine.

In the dimer series (d-A*p*A)$_{1and2}$ and (T*p*T)$_{1and2}$ (Table VII), the observed ^{2}E population for the dN*p*– unit is higher than that of the –*p*dN unit at low temperature. That is, the four dimers show a clear preference to populate the ^{2}E conformation, the preference being in general larger for the dN*p*– unit. At elevated temperatures, minor perturbations of the ^{2}E populations occur, although no definite trends can be observed. The ^{2}E populations of (d-A*p*A)$_1$ and (d-A*p*A)$_2$ are very similar, as are the ^{2}E populations of (T*p*T)$_1$ and (T*p*T)$_2$. This result suggests that there are no significant differences between the sugar conformations of the diastereoisomers of each dimer. Likewise, comparison of (d-A*p*A)$_{1and2}$ to d-ApA and (T*p*T)$_{1and2}$ to TpT shows that the sugar puckering of the phosphonate dimers is very similar, although not identical, to that of the diesters.

As indicated by Lee & Sarma (1975), the preferred conformers of the C(4′)–C(5′) bond may be gauche–gauche (*gg*),

[2] For a detailed description, please see the Appendix (supplementary material).

Table VI: Coupling Constants (J) in Hertz of the Sugar and Methylphosphonate Protons in Mono- and Dideoxyribonucleoside Methylphosphonates

compd	temp (°C)		coupling constant (Hz)												
			$J_{1',2'}$	$J_{1',2''}$	$J_{2',2''}$	$J_{2',3'}$	$J_{2'',3'}$	$J_{3',4'}$	$J_{4',5'}$	$J_{4',5''}$	$J_{5',5''}$	$J_{3',P}$	$J_{4',P}$	$J_{5',P}$	$J_{5'',P}$
dAp	26		8.0	6.1	−14.2	5.9	2.6	2.8	3.4	3.8	−13.6	7.6			
	75		7.6	6.0	−14.2	5.9	3.0	3.0	3.4	3.8	−12.7	8.0			
Tp	26		7.3	6.5	−14.2	7.2	3.5	3.9	3.6	4.9	−12.2	[a]			
	75		7.3	6.5	−14.2	6.9	3.8	3.9	3.7	5.0	−12.2	7.3			
$(CH_3pT)_1$	26		6.8	6.8	−14.0	6.7	4.6	4.3	4.9	3.0	−11.9		1.8	6.3	6.6
	75		7.3	6.8	−14.2	6.2	4.7	4.4	5.0	3.0	−11.9		1.8	6.3	6.6
(d-ApA)$_1$	26	dAp-	8.9	5.0	−14.5	6.3	1.3	2.4	3.0	3.0	−12.6	5.6			
		-pdA	7.4	6.3	−14.0	7.0	4.2	3.3	3.8	2.2	−11.0		1.8	4.5	6.3
	75	dAp-	8.5	5.8	−14.6	5.8	2.8	2.7	4.0	4.4	−12.6	5.9			
		-pdA	7.0	6.5	−14.0	6.3	4.6	4.2	4.8	2.5	−11.6		2.0	4.8	6.5
(d-ApA)$_2$	26	dAp-	8.7	5.6	−14.6	5.6	2.2	2.0	2.9	2.9	−12.6	6.3			
		-pdA	7.0	6.9	−14.0	6.0	5.9	3.2	3.4	3.2	−11.5		2.0	4.1	5.9
	75	dAp-	8.4	6.3	−14.6	6.3	2.5	2.7	3.9	3.9	−12.6	6.0			
		-pdA	6.7	6.8	−14.0	5.8	6.0	4.2	4.8	3.9	−12.2		2.0	4.8	6.0
(TpT)$_1$	26	Tp-	7.5	6.0	−14.0	6.7	2.5	3.0	3.4	4.3	−12.6	6.1			
		-pT	6.5	6.5	−14.0	5.7	5.7	4.7	5.1	2.4	−12.6		1.2	5.6	6.1
	75	Tp-	8.0	5.9	−14.1	6.6	2.9	3.3	3.7	4.7	−12.3	6.5			
		-pT	7.5	6.8	−14.1	6.8	4.8	4.4	4.8	3.1	−12.0		1.5	6.4	6.4
(TpT)$_2$	26	Tp-	7.3	5.8	−14.0	6.7	2.7	3.0	3.4	3.4	−12.6	6.9			
		-pT	6.7	6.7	−14.0	5.9	5.9	4.4	5.1	2.4	−11.6		1.2	5.6	6.1
	75	Tp-	7.8	6.1	−14.5	6.4	2.9	3.3	3.8	4.3	−12.6	6.5			
		-pT	7.4	6.8	−14.0	6.8	4.8	4.4	4.4	2.8	−11.8		1.4	6.3	6.3

[a] This coupling constant cannot be measured because the signal is under the HDO peak.

Table VII: Population Distribution of Conformers in dAp, Tp, $(CH_3pT)_1$, (d-ApA)$_{1 and 2}$, and (TpT)$_{1 and 2}$ [a]

compd	temp (°C)		sugar ring	backbone conformation		ϕ'	
			% ^{2}E	% gg	% $g'g'$		
dAp	26		74 (77)[b]	67 (71)[b]		203/277°	(202/278°)[b]
	75		72	67		204/276°	
Tp	26		64 (67)[c]	54 (57)[c]		[d]	(199/281°)[c]
	75		64	52		201/279°	
$(CH_3pT)_1$	26		60 (68)[e]	60 (59)[e]	58 (74)[e]		
	75		60	59	78		
(d-ApA)$_1$	26	dAp-	78 (78)[f]	79 (73)[f]		195/285°	(195/285°)[f]
		-pdA	69 (63)[f]	79 (87)[f]	68 (85)[f]		
	75	dAp-	75 (80)[f]	55 (59)[f]		196/284°	(197/283°)[f]
		-pdA	61 (63)[f]	66 (76)[f]	66 (76)[f]	196/284°	(197/283°)[f]
(d-ApA)$_2$	26	dAp-	81	81		197/283°	
		-pdA	70	84	72		
	75	dAp-	75	61		196/284°	
		-pdA	61	52	68		
(TpT)$_1$	26	Tp-	72 (70)[g]	62 (63)[g]		197/283°	(199/281°)[g]
		-pT	56 (63)[g]	64 (74)[g]	64 (82)[g]		
	75	Tp-	69 (67)[g]	55 (49)[g]		199/281°	(201/279°)[g]
		-pT	59 (66)[g]	60 (64)[g]	59 (77)[g]		
(TpT)$_2$	26	Tp-	72	71		199/281°	
		-pT	59	64	64		
	75	Tp-	69	58		199/281°	
		-pT	59	67	60		

[a] % ^{3}E = $J_{3',4'}/(J_{1',2'} + J_{3',4'}) \times 100$; % ^{2}E = 100 − % ^{3}E. % $gg = (13.7 - \Sigma)/9.7 \times 100$; $\Sigma = J_{4',5'} + J_{4',5''}$. % $g'g' = (25 - \Sigma)/20.8 \times 100$; $\Sigma = J_{5',P} + J_{5'',P}$. $^3J_{HP} = 18.1 \cos^2 \theta_{HP} - 4.8 \cos \theta_{HP}$; $\phi' = 240° \pm \theta$. [b] Corresponding results of dAp at 20 °C. [c] Corresponding results of Tp at 20 °C. [d] Not measurable. [e] Corresponding results of pT at 20 °C. [f] Corresponding results of d-ApA at 20 and 80 °C, respectively. [g] Corresponding results of TpT at 20 and 80 °C, respectively.

gauche–trans (gt), and trans–gauche (tg). The preferred conformers of the C(5′)–O(5′) bond may be gauche′–gauche′ ($g'g'$), gauche′–trans′ ($g't'$), and trans′–gauche′ ($t'g'$). These rotamer conformations are depicted in Figure 5. Because an unambiguous assignment of the two C(5′) protons is yet impossible, at present one cannot distinguish between gt and tg conformations or between $g't'$ and $t'g'$ conformations. Hence, one can only evaluate the contribution from gg vs. gt/tg or from $g'g'$ vs. $g't'/t'g'$ conformers. According to the equations developed by Lee & Sarma (1976), the gg and $g'g'$ populations can be computed as

$$\text{percentage population of } gg = (13.7 - \Sigma)/9.7$$

where $\Sigma = J_{H(4')-H(5')} + J_{H(4')-H(5'')}$ and

$$\text{percentage population of } g'g' = (25 - \Sigma')/20.8$$

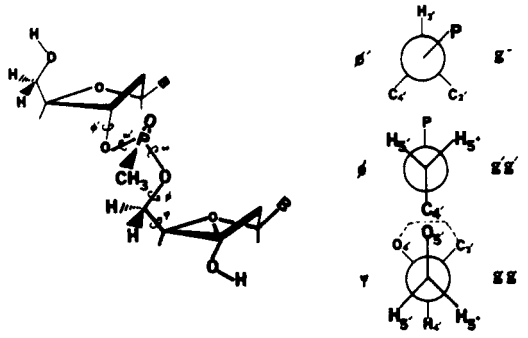

FIGURE 5: Diagram and nomenclature concerning the backbone conformation of d-ApA [the nomenclature is adopted from Sundaralingam (1973)].

where $\sum' = J_{H(5')-P} + J_{H(5'')-P}$. The computed populations of gg and $g'g'$ for the mono- and dideoxyribonucleoside methylphosphonates are compiled in Table VII. The data show that there is a general preference for gg and $g'g'$ conformers for all the monomers and dimers. Comparison of dAp, Tp, and $(CH_3pT)_l$ with the corresponding deoxyribonucleoside monophosphates shows that there is practically no change in the gg populations but there is a significant reduction in the $g'g'$ of $(CH_3pT)_l$ (16%). There is no effect of temperature on the gg populations of the methylphosphonate monomers.

Dimerization causes an increase in the gg populations of the dNp– units of both the adenine (12–14%) and thymine (8–17%) containing dimers at 26 °C. Comparison of the percent $g'g'$ in $(CH_3pT)_l$ with $(TpT)_{land2}$ shows an increase in the $g'g'$ conformer (8%). Increasing temperature depopulates the gg conformer, the effect being larger for $(d\text{-}ApA)_{land2}$ (17–32%) than for $(TpT)_{land2}$ (7–13%). On the other hand, there is very little effect (2–5%) on the $g'g'$ populations of these dimers with variation in temperature.

Comparison of the gg and $g'g'$ populations of the diastereoisomers of d-ApA or TpT shows very little change in the percentage of either the gg (2–9%) or $g'g'$ (0–4%) conformers. The gg populations of $(d\text{-}ApA)_{land2}$ and $(TpT)_{land2}$ are very similar to those of d-ApA and TpT, respectively. However, the phosphonate dimers show up to 18% reduction in the percent $g'g'$ population compared to the parent dinucleoside monophosphate.

For analysis of the rotamer distribution of bond angle ϕ' (Figure 5), again the conventional approach is based upon a three-rotamer model such as the P–O(3′) bond trans to C(3′)–C(4′) (g^- or gt; $\phi' = 180°$), the P–O(3′) bond trans to C(3′)–C(2′) (g^+ or tg; $\phi' = 300°$), and the P–O(3′) bond trans to C(3′)–H(3′) (t or gg; $\phi' = 60°$). Previous studies on this bond rotation of monomers, dimers, and polymers based on $^3J_{HP}$ data (Davies & Danyluk, 1975; Lee & Sarma, 1975; Cheng & Sarma, 1977; Alderfer & Ts'o, 1977) and on $^3J_{CP}$ data (Alderfer & Ts'o, 1977) indicated that the t conformer is most likely to be unpopulated and the population can be described as in a rapid equilibrium between a modified g^- ($\phi' \approx 200°$) state and a modified g^+ ($\phi' \approx 280°$) state. In adopting this approach and using the Karplus equation (Lee & Sarma, 1976)

$$^3J_{HP} = 18.1 \cos^2 \theta_{HP} - 4.8 \cos \theta_{HP}$$

two sets of $H_{3'}$–$C_{3'}$–$O_{3'}$–P dihedral angles can be computed for these phosphonate mono- and dinucleotides as shown in Table VII. As an example of the computation, the value of $^3J_{H(3)-P}$ of dAp would yield a θ_{HP} of ±37 and ±122°. The conformation of $\theta_{HP} = 0°$ is equivalent to that of $\phi' = 240°$; model studies indicate that the conformational state of $\phi' = 240 \pm 122°$ should be sterically forbidden, and thus it was not included in the original three-rotamer model. The remaining allowable conformational state for dAp becomes $\phi' = 240 \pm 37°$, i.e., 203 or 277°, as shown in Table VII.

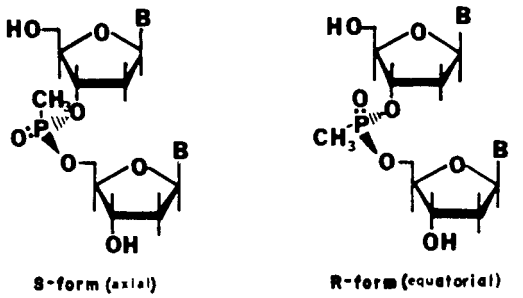

FIGURE 6: Absolute configuration of d-NpN′ (N and N′ = T or A): the S form (pseudoaxial) vs. the R form (pseudoequatorial).

Configuration of the Methylphosphonate Groups of $(d\text{-}ApA)_{land2}$. As shown in Figure 6, when the dimers are in a stacked conformation, the phosphonate methyl group of one diastereoisomer would assume a pseudoaxial position (S form) and the phosphonate methyl group of the other isomer would assume a pseudoequatorial position (R form). In the axial position, the methyl group is directed toward the base stacking region as well as the $H_{3'}$ of the dNp– unit of the dimer, while in the equatorial position the methyl group is directed away from the stack and from other atoms of the dimer. Therefore, a larger NOE effect on the PCH_3 may be expected when the $H_{3'}$ of the dNp– unit of the axial dimer (S form) is irradiated. An NOE experiment was carried out on the two diastereoisomers of d-ApA since this dimer shows the largest degree of base stacking. Only $(d\text{-}ApA)_l$ showed an NOE on the PCH_3 group. Therefore, the PCH_3 group in this isomer is assigned the axial position or S configuration, while the PCH_3 group in isomer 2 is assigned the equatorial position or R configuration. This conclusion is supported by the chemical shift data presented in Table I which show that at low temperatures the PCH_3 resonances of isomer 1 occur at slightly higher field than the PCH_3 resonances of isomer 2. This slight shielding effect could reflect the closer proximity of the methyl group in isomer 1 to the base stacking region of the dimer.

Concluding Remarks. The results of the present ^{1}H NMR investigation show that the dinucleoside methylphosphonates adopt stacked conformations in aqueous solution similar to those of the dinucleoside monophosphates and dinucleoside alkyl phosphotriesters. The configuration of the phosphonate methyl group exerts an influence on the stacking mode of the bases. Thus, for the dimer d-ApA the stacking is slightly greater in isomer 1 (or S form) than in isomer 2 (or R form). The base stacking patterns in both isomers are very similar to that in the dinucleoside monophosphate d-ApA with the stacking of isomer 1 being identical with that of the diester. These results are in agreement with the previous results derived from UV and CD measurements on the dimers (Miller et al., 1979b). The conformation of the sugar–phosphonate backbone of the methylphosphonate dimers defined by the puckering of the deoxyribofuranose rings and the rotations about ψ, ϕ, and ϕ' is very similar to that of the dinucleoside monophosphates. Again, small differences are observed between the diastereoisomers of each dimer.

These results lead to the conclusion that the methylphosphonate analogues are good models for dinucleoside monophosphates and that alteration of the internucleotide linkage does not significantly affect the overall conformational properties of the dimers. The result is not unexpected, since replacement of the nonesterified oxygen of the phosphodiester linkage with a methyl group represents only a small increase

in steric bulk at this position. X-ray crystallographic results on the model compounds dimethyl 1-hydroxycyclododecyl- and 1-hydroxycyclotridecylphosphonates (Samuel & Weiss, 1969) show that the bond angles about the phosphonate group are in the same range as those found in the dinucleoside monophosphate ApU (Seeman et al., 1976) and the ethyl of adenosine nucleoside ethyl phosphotriester cyclic 3′,5′-monophosphate (Cotton et al., 1975). The small changes which are observed could result from changes in rotation about ω and ω' (see Figure 5).

The differences in the conformation between the diastereoisomers of each dimer could also be influenced by differences in solvation of these two isomers. Thus, the hydrophobic axial methyl group in (d-A*p*A)$_1$ is situated near the hydrophobic base stacking region of the dimer and could be included in this region. This inclusion would tend to stabilize the base stacking interaction in the dimer. The equatorial methyl group of isomer 2, on the other hand, may be expected to destabilize the base stacking interaction since this hydrophobic group is directed away from the base stacking region. This effect could account for the more open stack observed for isomer 2.

Acknowledgments

The authors express their deep appreciation to Drs. Claude Giessner-Prettre and Bernard Pullman for providing the program, to James R. Kast as well for his aid in computer programming, and to the Mid-Atlantic NMR Facility Center (University of Pennsylvania, Philadelphia, PA) for use of Varian HR-220 and Bruker WH 360 NMR spectrometers.

Supplementary Material Available

An appendix ("A Computer Program for Calculating the Mutual Shielding Effects of Two Adenine Bases" by C. Giessner-Prettre, B. Pullman, L. S. Kan, J. R. Kast, and P. O. P. Ts'o) for the detailed calculation of the shielding effect of adenine bases (8 pages). Ordering information is given on any current masthead page.

References

Alderfer, J. L., & Ts'o, P. O. P. (1977) *Biochemistry 16*, 2410.

Altona, C., & Sundaralingam, M. (1973) *J. Am. Chem. Soc. 95*, 2333.

Cheng, D. M., & Sarma, R. H. (1977) *J. Am. Chem. Soc. 99*, 7333.

Cheng, D. M., Kan, L. S., Ts'o, P. O. P., Giessner-Prettre, C., & Pullman, B. (1980) *J. Am. Chem. Soc. 102*, 525.

Cotton, F. A., Gillen, R. G., Gohil, R. N., Hazen, E. E., Jr., Kirchner, C. R., Nagyvary, J., Rouse, J. P., Stanislowski, A. G., Stevens, J. D., & Tucker, P. W. (1975) *Proc. Natl. Acad. Sci. U.S.A. 72*, 1335.

Davies, D. B., & Danyluk, S. S. (1975) *Biochemistry 14*, 543.

Giessner-Prettre, C., & Pullman, B. (1968) *C. R. Hebd. Seances Acad. Sci., Ser. C 266*, 933.

Giessner-Prettre, C., Pullman, B., Borer, P. N., Kan, L. S., & Ts'o, P. O. P. (1976) *Biopolymers 15*, 2277.

Kan, L. S., Barrett, J. C., Miller, P. S., & Ts'o, P. O. P. (1973a) *Biopolymers 12*, 2225.

Kan, L. S., Barrett, J. C., & Ts'o, P. O. P. (1973b) *Biopolymers 12*, 2409.

Kondo, N. S., Fang, K. N., Miller, P. S., & Ts'o, P. O. P. (1972) *Biochemistry 11*, 1991.

Lee, C. H., & Sarma, R. H. (1975) *J. Am. Chem. Soc. 97*, 1225.

Lee, C. H., & Sarma, R. H. (1976) *J. Am. Chem. Soc. 98*, 3541.

Miller, P. S., Fang, K. N., Kondo, N. S., & Ts'o, P. O. P. (1971) *J. Am. Chem. Soc. 93*, 6657.

Miller, P. S., McParland, K., & Ts'o, P. O. P. (1979a) 11th International Congress of Biochemistry, Abstract 02-5-H59.

Miller, P. S., Yano, J., Yano, E., Carroll, C., Jayaraman, K., & Ts'o, P. O. P. (1979b) *Biochemistry 18*, 5134.

Samuel, G., & Weiss, R. (1969) *Tetrahedraon Lett. 33*, 2803.

Seeman, N. C., Rosenberg, J. M., Suddath, F. L., Kim, J. J. P., & Rich, A. (1976) *J. Mol. Biol. 104*, 109.

Sundaralingam, M. (1973) *Jerusalem Symp. Quantum Chem. Biochem. 5*, 617.

Ts'o, P. O. P., Kondo, N. S., Schweizer, M. P., & Hollis, D. P. (1969) *Biochemistry 8*, 997.

Ts'o, P. O. P., Barrett, J. C., Kan, L. S., & Miller, P. S. (1973) *Ann. N.Y. Acad. Sci. 222*, 290.